

## Sensitive measurement of trace amounts of promethazine hydrochloride at MWCNT-COOH nanostructures modified pencil graphite electrode based on charge transfer complex formation

Ali Mohammad Amani<sup>a, b, c, \*</sup>, Mohammad Hassan Motaghedifard<sup>d, \*</sup>, Ebrahim Honarmand<sup>e</sup>, Mahnaz Motmaen<sup>f</sup>,  
Younes Ghasemi<sup>a, b</sup>, Amir Savardashtaki<sup>g</sup> & Ali Arabi Monfared<sup>h</sup>

<sup>a</sup>Department of Medical Nanotechnology, School of Advanced Medical Sciences and Technologies,  
Shiraz University of Medical Sciences, Shiraz, Iran  
Email: ali\_amani1383@yahoo.com

<sup>b</sup>Pharmaceutical Sciences Research Center, Shiraz University of Medical Sciences, Shiraz, Iran

<sup>c</sup>Department of Chemistry Shiraz University of Technology Shiraz, Iran

<sup>d</sup>Young Researchers and Elites Club, Qom Branch, Islamic Azad University, Qom, Iran  
Email: mhmf1359@yahoo.com

<sup>e</sup>Department of Chemistry, Faculty of Science, University of Qom, Qom, 37161-46611, I.R. Iran

<sup>f</sup>Department of Analytical Chemistry, Faculty of Chemistry, University of Kashan, Kashan, P.O. Box 87317-51167, IR Iran

<sup>g</sup>Department of Medical Biotechnology, School of Advanced Medical Sciences and Technologies,  
Shiraz University of Medical Sciences, Shiraz, Iran

<sup>h</sup>Central Research Laboratory, Shiraz University of Medical Sciences, Shiraz, Iran

Received 19 June 2017; re-revised and accepted 28 May 2018

Functionalized multiwalled carbon nanotubes (MWCNT-COOH) pencil graphite electrode has been fabricated to detect trace amounts of promethazine hydrochloride (PMZ). The modified electrode has been applied in Fe<sup>2+/3+</sup> probes, hydroquinone probe and PMZ solutions by cyclic voltammetry and electrochemical impedance spectroscopy. The MWCNT-COOH/PGE shows better response for electrooxidation of PMZ as compared to MWCNT/PGE based on charge transfer complex formation. Two linear dynamic ranges are seen between 0.05 and 275.0  $\mu\text{M}$  with the limit of detection of 5.61 nM in the analysis of PMZ by differential pulse voltammetry. The diffusion coefficient ( $D$ ,  $\text{cm}^2 \text{s}^{-1}$ ) and the kinetic parameters such as the electron transfer coefficient ( $\alpha$ ), and the ionic exchanging current density ( $i_0$ ) for PMZ have also been determined using electrochemical approaches. The modified electrode has been applied to determine PMZ in real sample with satisfactory results.

**Keywords:** Electrochemistry, Electroanalytical chemistry, Electrooxidation, Multiwalled carbon nanotubes, Carbon nanotubes, Nanotubes, Pencil graphite electrodes, Graphite electrodes, Prometazine hydrochloride

Since the discovery of carbon nanotubes (CNTs) by Iijima<sup>1</sup>, they have attracted tremendous research interest in many areas due to their unique structural, mechanical, electronic, and chemical properties.<sup>2</sup> The subtle electronic properties of CNTs reveal that they have the ability to promote electron-transfer reactions when used as an electrode material in electrochemical reactions.<sup>3,4</sup>

Usually CNTs need to be purified and functionalized before use to eliminate amorphous carbon and other metal catalyst.<sup>5</sup> Amongst the purification methods, oxidation is regarded as an effective method.<sup>6-11</sup> Earlier, the chemically oxidized CNTs were synthesized with oxidant reagents such as H<sub>2</sub>SO<sub>4</sub>, HNO<sub>3</sub><sup>12</sup>, HCl, H<sub>2</sub>O<sub>2</sub>, O<sub>2</sub><sup>10,13</sup> etc., in presence of large amounts of chemicals and at high temperatures.

The oxidation process also has many other disadvantages such as environmental pollution, high cost, complexity of the operation process, and difficulty in controlling. Recently, electrochemical methods have been reported to purify and functionalize raw CNTs with electrochemical oxidization reaction in electrolyte solution by cyclic voltammetry<sup>5,14</sup>, and constant-current<sup>15</sup> or constant-potential<sup>16</sup> methods.

In a previous work<sup>17</sup>, we have investigated the electrochemical behavior of promethazine HCl on the surface of MWCNT-carbon paste electrode. In comparison with other carbon based electrodes, PGEs have some advantages such as high electrochemical reactivity, low background current, wide potential window, chemical inertness, commercial availability,

good mechanical rigidity, disposability, low costs, low technology, easy modification and miniaturization<sup>18–20</sup>. The PGE, when combined with a more highly sensitive and accurate voltammetric technique such as square-wave or differential pulse voltammetry, can lead to an attractive trace analysis technique. Additionally, it was reported that pencil lead electrodes offer a renewable surface, which is simpler and faster than polishing procedures usually required for solid or paste electrodes, and results in good reproducibility for the individual surfaces<sup>18</sup>. Therefore, in view of the above benefits, the PGE was selected in the present study to increase sensitivity and reproducibility of electrochemical response of PMZ.

PMZ, which belongs to the phenothiazine group, is widely used as an antihistaminic for the symptomatic relief of hypersensitivity reactions and for enhancing the analgesic, anesthetic and sedative effect of other drugs<sup>21,22</sup>. On the other hand, PMZ can cause adverse effects in body such as endocrinal and cardiac problems, reproductive alterations, occasional hypotension, etc.<sup>23</sup> Therefore its determination in commercial formulations is extremely important. Some analytical methods such as chemiluminescence,<sup>24</sup> high performance liquid chromatography<sup>25,26</sup> and capillary zone electrophoresis<sup>27</sup> have been previously reported for the determination of PMZ. Most of these methods are time consuming, complicated and also require expensive instrumentation. In recent years, electroanalytical methods are being applied more to determine PMZ, since these are simple, inexpensive, and require relatively short analysis times<sup>28,29</sup>.

In the present study, an electrochemically oxidized MWCNTs modified pencil graphite electrode (PGE) was used to construct a sensor for the determination of PMZ in pharmaceutical formulations. Herein, firstly, multiwalled carbon nanotubes were oxidized and functionalized through cyclic voltammetry method at the sweep potential range of 0.0–1.6 V and 30 continuous cycles in 0.05 M H<sub>2</sub>SO<sub>4</sub> solution. Then, the surface functionalisation was confirmed by electrochemical techniques. Finally, the modified electrode was used for the detection of PMZ in buffer solution.

## Materials and Methods

Voltammetric measurements were made on a potentiostat/galvanostat (SAMA 500, electroanalyzer system, I.R. Iran). The EIS measurements were made using an Autolab Potentiostat/Galvanostat PGSTAT30 (Eco Chemie, Utrecht, Netherlands)

controlled by the Frequency Response Analyzer (FRA) 4.9 software which was adapted to a conventional three-electrode system. The working electrode was carboxylated multiwalled carbon nanotube pencil graphite electrode (MWCNT-COOH@PGE) and the auxiliary and reference electrodes were platinum wire and Ag/AgCl (3.0 M of KCl) electrodes, respectively. A Metrohm digital pH meter (model 691) was used to adjust pH of buffer solutions. All electrochemical measurements were carried out at 25±0.5 °C. SEM images were obtained on a Philips XL-30ESEM and TEM images were recorded on a Philips EM208S transmission electron microscope with an accelerating voltage of 100 kV.

PMZ, H<sub>2</sub>SO<sub>4</sub>, H<sub>3</sub>PO<sub>4</sub>, NaOH and other materials were purchased from Sigma-Aldrich and used without purification. Their solutions were prepared using distilled water (0.055 µS). Multiwalled carbon nanotubes (MWCNTs) were purchased from the Chinese Academy of Sciences (outer dia. 10–20 nm, length <1–2 µm and purity >95%). PMZ solutions were prepared immediately prior to use. Phosphate buffer solutions at different pH values were prepared by titrating 0.1 M H<sub>3</sub>PO<sub>4</sub> with saturated solution of NaOH.

### Electrodes preparation

A suspension of MWCNTs in dimethyl formamide (DMF) was prepared by dispersing 1.0 mg MWCNTs in 10.0 mL of DMF. The suspension was ultrasonically dispersed for 1 h. Separately, a PGE was hand polished using polishing microcloth treated with 0.05 mm alumina powder for several minutes and then ultrasonically cleaned with ethanol solution (50%, v/v in water) to remove any physically adsorbed impurity. Then, the electrode was rinsed thoroughly with doubly distilled water. For modification, 20 µL of the stable MWCNT suspension was dropped onto the surface of PGE and dried in a hot air flow at 50 °C. Then, the MWCNT@PGE was washed with doubly distilled water, dried at room temperature and applied for electrochemical experiments.

### Electrooxidation of MWCNTs

For electrooxidation of the carbon nanotubes, the MWCNT@PGE was immersed in 0.05 M H<sub>2</sub>SO<sub>4</sub> solution and the potential was cycled 20 times between +0.00 V and +1.50 V at a scan rate of 50 mV/s. After this treatment, the functionalized sensor was washed with doubly distilled water and studied in electroactive probe solutions to confirm the presence of MWCNT-COOH.

## Results and Discussion

### Electrochemical oxidation of MWCNTs in 0.05 M H<sub>2</sub>SO<sub>4</sub>

Electrochemical oxidation of MWCNTs was first reported by Crooks and co-workers<sup>16,30</sup>, in which they observed that MWCNTs can be etched at potentials more positive than 1.7 V versus Ag/AgCl (3 M NaCl) in an aqueous 0.1 M KCl electrolyte solution. However in this study, the MWCNTs were electrochemically oxidized by potential cycling in 0.05 M H<sub>2</sub>SO<sub>4</sub> between +0.0 V and +1.5 V at a scan rate of 50 mV/s. Figure 1 shows twenty continuous cyclic voltammograms for the electrochemical oxidation of MWCNTs in 0.05 M H<sub>2</sub>SO<sub>4</sub>. A broad anodic peak with three climaxes appears in the potential range from +1.05 V to +1.40 V on the first scan. The peak potentials dwindle during the subsequent cycles until a minimum value is finally reached. This indicates that the oxidation of MWCNTs at high potential is efficient and completely irreversible.

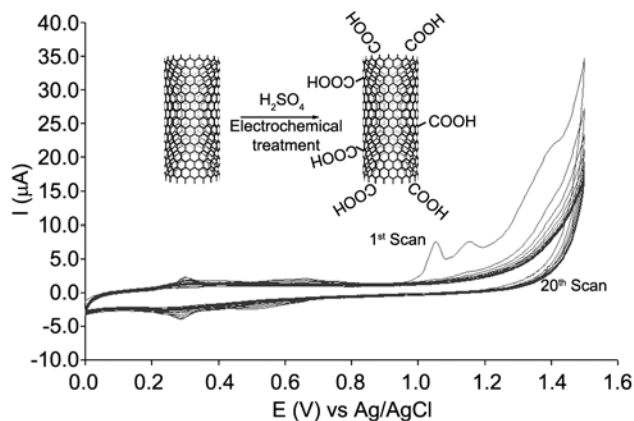


Fig. 1 — Successive CVs of MWCNT@PGE in 0.05 M of H<sub>2</sub>SO<sub>4</sub> at a scan rate 25 mV/s.

### Morphology of MWCNT and MWCNT-COOH

The morphology of carbon nanotubes before and after electrochemical oxidation was investigated using scanning electron microscope (SEM) and transmission electron microscopy (TEM). The results of SEM and TEM are shown in Fig. 2a and 2b. The images show that the original MWCNTs (Fig. 2a) were smooth, with closed endpoints, curved and dark colored. However, after oxidation, the endpoint of COOH-MWCNTs was found to be open, some of the MWCNTs were cut into shorter ones, the surface was eroded and the MWCNTs were brighter in color (Fig. 2b). These images confirm that electrochemical oxidation can purify and erode the MWCNTs.

### Electrochemical study of MWCNT-COOH@PGE

Cyclic voltammetry (CV) was used to study the effect of the modifier. The CVs for 1.0 mM K<sub>4</sub>[Fe(CN)<sub>6</sub>]/K<sub>3</sub>[Fe(CN)<sub>6</sub>] in 0.1 M KCl buffer solution on the bare PGE, MWCNT@PGE and MWCNT-COOH@PGE are shown in Fig. 3. The quasi-reversible one-electron redox behavior of Fe<sup>+2/+3</sup> ions was observed on the bare PGE with a peak separation ( $\Delta E_p$ ) of 0.322 V at the scan rate of 50 mV/s. With the MWCNTs@PGE, the peak currents of Fe<sup>+2/+3</sup> increased about 3.12 times as compared to that of bare PGE, while the  $\Delta E_p$  decreased to 0.091 V. For MWCNT-COOH@PGE, decreasing of redox current is noteworthy, which can be attributed to the presence of carboxylic ions on the surface of MWCNTs. Carboxylic ions acts as a barrier against diffusion of Fe<sup>+2/+3</sup> ions to the surface of electrode. The results are summarized in Table S1 (Supplementary Data).

The electrochemical impedance spectroscopy (EIS) was used to characterize electrochemical differences

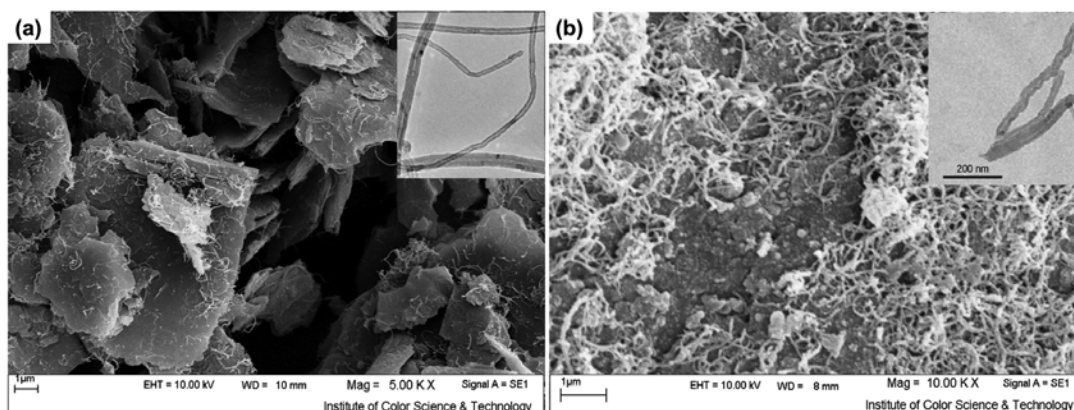


Fig. 2 — Typical SEM images of (a) MWCNT, and, (b) MWCNT-COOH nanostructures at the surface of PGE. [Inset: TEM images of MWCNT and MWCNT-COOH nanostructures].

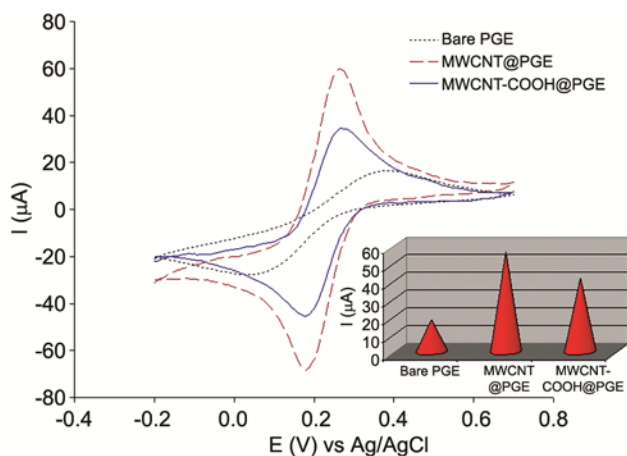


Fig. 3 — Cyclic voltammograms of bare PGE, MWCNT@PGE and MWCNT-COOH@PGE in the presence of 1.0 mM of  $K_4Fe(CN)_6/K_3Fe(CN)_6$  in 0.1 M of KCl, and scan rate of 50 mV/s.

between PGE, MWCNT@PGE and MWCNT-COOH@PGE. The measurements were made in Faradaic mode, using the redox probe  $K_4[Fe(CN)_6]/K_3[Fe(CN)_6]$  in 0.1 M KCl solution to monitor the variations of the charge transfer resistance ( $R_{ct}$ ) between solution and electrode surface (Fig. 4). For better analysis and fit view of results, an equivalent circuit model was used. Results showed a minor  $R_{ct}$  at MWCNT@PGE (Fig. 4 (curve 2)) compared to bare PGE (Fig. 4 (curve 1)), which indicates a significant increase in the rate of charge transfer. For bare PGE,  $R_{ct}$  was calculated as 11.105 k $\Omega$  by fitting of its Nyquist diagram on  $[R_s(Q[R_{ct}W])]$  model. After modification with MWCNT, the  $R_{ct}$  decreased to 4.304 k $\Omega$  (by fitting to  $[R_s(Q[R_{ct}W])]$  model) which is much lower than that on the bare PGE (Fig. 4 (curve 2)). Oxidation of MWCNTs caused an increase in the value of  $R_{ct}$  to 5.641 k $\Omega$  according to fitting data on the  $[R_s(Q[R_{ct}W])]$  model (Fig. 4 (curve 3)). This change can be attributed to the presence of carboxylic ions on the surface of the MWCNTs which creates a barrier against diffusion of  $Fe^{+2/+3}$  ions to the surface of electrode. The results are summarized in Table S2 (Supplementary Data).

Cyclic voltammetry was also carried out in hydroquinone (PBQ/H<sub>2</sub>Q) solution. In presence of an inert probe such as PBQ/H<sub>2</sub>Q, the behavior of MWCNT-COOH was studied. The CVs of the PGE, MWCNT@PGE and MWCNT-COOH@PGE in 5.0 mM PBQ/H<sub>2</sub>Q in phosphate buffer solution (pH 6.0) is shown in Fig. 5. In this case, due to hydrogen bonding between the carboxylic group and PBQ probe, the oxidation current of PBQ was found to be a little higher than normal MWCNTs.

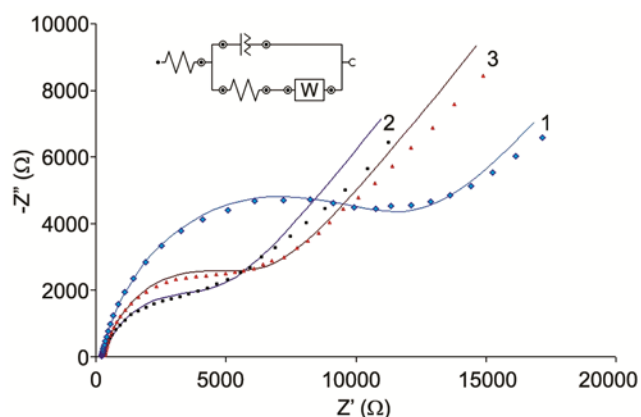


Fig. 4 — Nyquist plots for bare PGE (1), MWCNT@PGE (2), and, MWCNT-COOH@PGE (3) in the presence of 1.0 mM of  $K_4Fe(CN)_6/K_3Fe(CN)_6$  in 0.1 M of KCl. [DC potential: +300 mV; AC amplitude: 5.0 mV; frequency range: 10 kHz to 100 mHz].

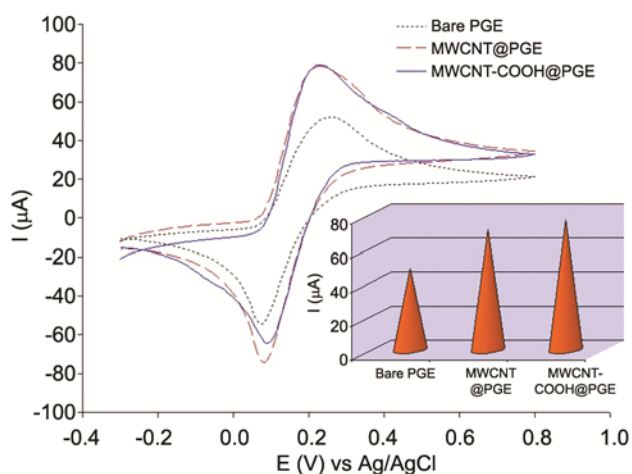


Fig. 5 — Cyclic voltammograms of bare PGE, MWCNT@PGE and MWCNT-COOH@PGE in the presence of 5.0 mM of PBQ/H<sub>2</sub>Q in 0.1 M of KCl, and scan rate of 50 mV/s.

#### Electrochemical Behavior of promethazine HCl on MWCNT-COOH

Figure 6a depicts the electrochemical behavior of 100.0  $\mu$ M PMZ at the surface of bare PGE, MWCNT@PGE and MWCNT-COOH@PGE. As can be seen from CV curves, the oxidation peak of PMZ at MWCNT-COOH@PGE was a triplet (585, 792 and 904 mV) and greater than the doublet oxidation peak at MWCNT@PGE (594 and 800 mV). In this case, the response on bare PGE was a singlet and was very weak (678 mV). This clearly demonstrates the favorable signal-enhancing effect (20.3 times magnification) with a  $-93$  mV decrease of overpotential as compared to bare PGE at the MWCNT-COOH@PGE. On the other hand, the DPVs obtained for PMZ at MWCNT-COOH@PGE

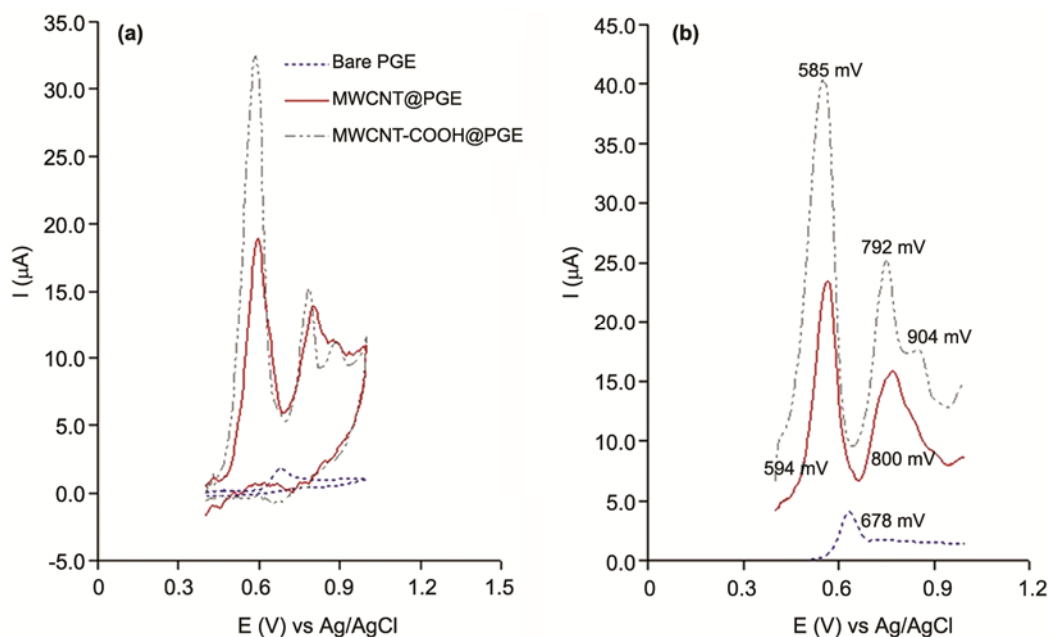


Fig. 6 — (a) CVs of bare PGE, MWCNT@PGE and MWCNT-COOH@PGE in the presence of 100.0  $\mu\text{M}$  PMZ at pH 4.0 of 0.1 M PBS, and, (b) DPVs of bare PGE, MWCNT@PGE and MWCNT-COOH@PGE in the presence of 100.0  $\mu\text{M}$  PMZ at pH 4.0 of 0.1 M PBS.

in PBS (pH 4.0) clearly depict a triplet and sharp oxidation of PMZ in comparison to MWCNT@PGE and bare PGE (Fig. 6b). The multiplicity of peaks obtained at the electrode surface indicates more interaction with the surface based on hydrogen bonding and charge transfer complex formation<sup>31</sup> between carboxylated MWCNTs and PMZ, which drives the electrochemical oxidation process of PMZ towards completion. In this case, the oxidation current is increased.

#### Optimization of various factors

To study the effect of pH on the oxidation process of PMZ, the DPV responses of 125.0  $\mu\text{mol/L}$  PMZ at the MWCNT-COOH@PGE surface was obtained at differential pH values ranging from 2.0–9.0 and a scan rate of 25 mV/s (Fig. 7). Result shows that the peak potential of the PMZ was pH dependent and decreased with increasing pH according to the Nernst equation. A slope of  $-36.7$  mV/pH unit at 25  $^{\circ}\text{C}$  was obtained in accordance with the Nernstian value for a tri-electron, two-proton process in pH range 2.0–9.0 in the electrochemical reaction. Also, it can be seen that the maximum value of the peak current appeared at pH 4.0 (Fig. 7), hence this value was selected throughout the experiments.

The DPV method was used to improve the sensitivity of MWCNT-COOH@PGE for the determination of PMZ. The optimum instrumental

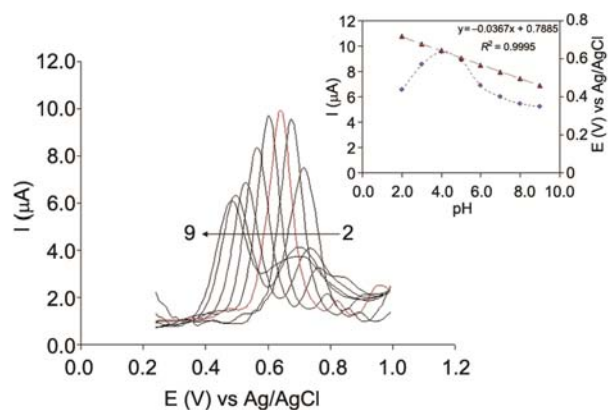


Fig. 7 — DPVs of 125.0  $\mu\text{M}$  PMZ at various buffered pHs (pH 2 to 9), at a scan rate of 25.0  $\text{mV s}^{-1}$ . [Inset: variation of  $I$  ( $\mu\text{A}$ ) versus pH and electrochemical potential,  $E_{\text{pa}}$  (V) versus pH].

conditions were obtained from a study of the variation of the peak current with pulse width, scan rate, H step potential and pulse height. During the investigations, each variable was changed while the other variables were kept constant. The results showed that for voltammograms of a relatively high sensitivity and well-shaped waves with a relatively narrow peak width, a scan rate of 25 mV/s, pulse width of 0.08 s, H step potential of 4.0 mV and pulse height of 50 mV were necessary.

The effect of scan rate ( $\nu$ ) on oxidation process of 75.0  $\mu\text{M}$  of PMZ was studied on MWCNT-COOH@PGE (Fig. 8) in PBS (pH 4.0) and sweep rates between 25



and 150 mV/s. For totally irreversible diffusion controlled process<sup>32</sup>.  $I_p = 2.69 \times 10^5 n^{3/2} A D^{1/2} C v^{1/2}$  where  $D$  ( $\text{cm}^2/\text{s}$ ) is the diffusion coefficient,  $A$  ( $\text{cm}^2$ ) is the surface area of electrode and  $C$  (M) is the concentration of reagent. In the scan rate range of 25.0–150.0 mV/s, the oxidation peak current increased linearly with the square root of scan rate, which is typical of a diffusion-controlled process of PMZ at the MWCNT-COOH@PGE (Fig. 8 (Inset a)). Therefore, the linear regression equation for PMZ was found to be:  $I_{pa} = 0.867 v^{1/2} + 2.963$ ,  $R^2 = 0.9934$ . Inset b of Fig. 8 shows the Tafel plot ( $E$  versus  $\log I$ ), plotted by using the data derived from the rising part of the current-voltage curve at a scan rate of 85 mV/s. The number of electrons involved in the rate-determining step ( $n_a$ ), charge transfer coefficient ( $\alpha$ ) and the ionic exchange current ( $i_0$ ) can be estimated from the slope and the intercept, respectively, of the Tafel plot. A Tafel slope of 0.124 V per decade was obtained, indicating that assuming a one-electron process involved in the rate-determining step, the charge transfer coefficient ( $\alpha$ ) was 0.53. Also, the value of  $i_0$  was found to be  $1.66 \mu\text{A}/\text{cm}^2$  from the intercept of the Tafel plot.

#### Oxidation of PMZ by chronocoulometry

To evaluate the diffusion coefficient in electrooxidation of PMZ at MWCNT-COOH@PGE, the chronocoulograms of PMZ solutions were plotted in the concentrations ranging from 0.04–0.24 mM, using a potential step of 650 mV (Fig. 9). For PMZ as

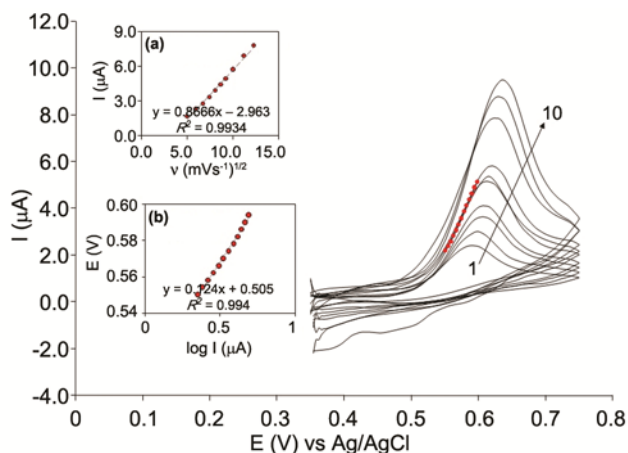


Fig. 8 — CVs obtained at MWCNT-COOH@PGE in a 0.1 M PBS (pH 4.0) containing  $75.0 \mu\text{M}$  PMZ at different scan rates. [Curves 1–10 correspond to scan rates of 25, 35, 45, 55, 65, 75, 85, 100, 125 and 150 mV/s respectively. Insets: (a) Variation of the electrocatalytic currents versus square root of the scan rate, and, (b) Variation of the anodic peak potential versus  $\log I$ ].

an electroactive material with a diffusion coefficient  $D$ , the current for the electrochemical reaction (at a mass transport limited rate) is described by the Cottrell equation<sup>32</sup>,  $Q = 2nFAD^{1/2} t^{1/2} C \pi^{-1/2}$  where  $D$  ( $\text{cm}^2 \text{ s}^{-1}$ ) and  $C$  ( $\text{mol cm}^{-3}$ ) are the diffusion coefficient and the bulk concentration, respectively. Under diffusion limited transport (mass transport), a plot of  $Q$  versus  $t^{1/2}$  ( $\text{s}^{1/2}$ ) will be linear, and the value of  $D$  can be extracted from the slope. Figure 9(a&b) shows the fitted experimental plots for different concentrations of PMZ. The slopes of the resulting linear plots were plotted versus the PMZ concentration, and the value of  $D$  was found to be  $3.7 \times 10^{-6} \text{ cm}^2/\text{s}$ .

#### Calibration curve and limit of detection

Due to the higher sensitivity of differential pulse method as compared to cyclic voltammetry for measurement of current, DPV was used for the determination of PMZ in the present work (Fig. 10). The plot of peak current versus PMZ concentration comprised two linear segments with slopes of 0.214 and  $0.053 \mu\text{A}/\mu\text{M}$  in the concentration ranges of  $0.05$ – $62.5 \mu\text{M}$  and  $62.5$ – $275.0 \mu\text{M}$ , respectively (Fig. 10 (Inset)). The decrease in sensitivity (slope) of the second linear segment is likely to be due to kinetic limitations. The lower detection limit,  $C_M$ , was obtained as  $5.61 \text{ nM}$  from the equation  $C_M = 3S_b/m$ , where  $S_b$  is the standard deviation of the blank response ( $\mu\text{A}$ ) and  $m$  is the slope of the calibration plot. The response of MWCNT-COOH@PGE to PMZ is comparable with previous reported studies summarized in Table S3 (Supplementary Data).

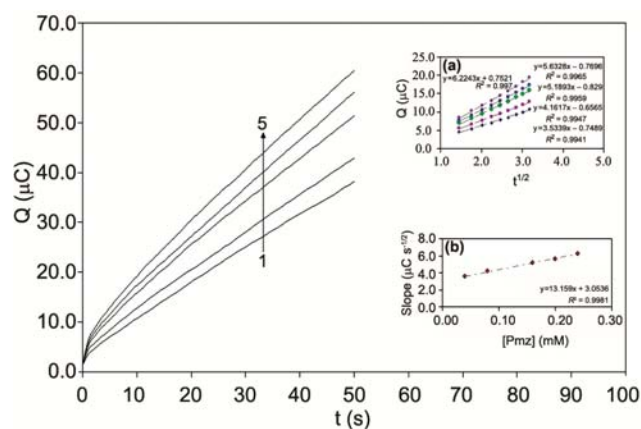


Fig. 9 — Charge-time curves obtained at MWCNT-COOH@PGE in 0.1 M PBS (pH 4.0) for different concentrations of PMZ. [Plots 1–5 correspond to 40.0, 80.0, 160.0, 200.0 and  $240.0 \mu\text{M}$  PMZ, respectively. Insets: (a) Plots of  $Q$  versus  $t^{1/2}$  obtained from chronocoulograms 1–5, and, (b) Plot of the slopes against PMZ concentration].

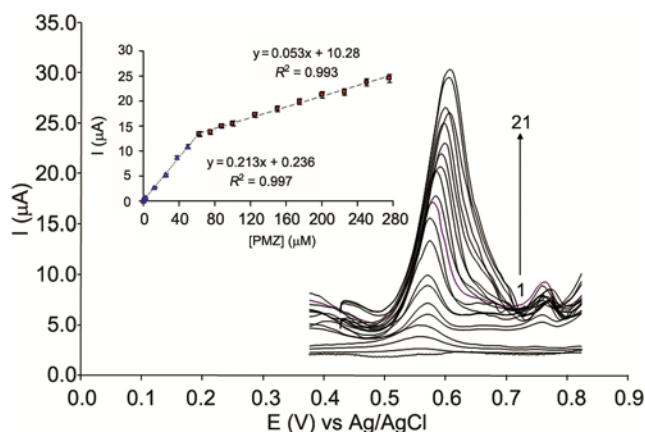


Fig. 10 — DPVs of varying concentrations of PMZ at MWCNT-COOH@PGE in 0.1 M PBS (pH 4.0). [Curves 1-21 correspond respectively to 0.0, 0.05, 0.1, 0.5, 1.25, 2.5, 12.5, 25.0, 37.5, 50.0, 62.5, 75.0, 87.5, 100.0, 125.0, 150.0, 175.0, 200.0, 225.0, 250.0 and 275.0  $\mu\text{M}$  of PMZ. Inset shows the plots of the electrocatalytic peak current as a function of PMZ concentration].

The stability and reproducibility of MWCNT-COOH@PGE was investigated by DPV measurements of 40.0  $\mu\text{M}$  PMZ. The relative standard deviation (RSD, %) of peak current and oxidation peak potential of PMZ for ten successive assays were 1.65% and 0.48%, respectively, showing good repeatability of the electrode response. In addition, the reproducibility of modified electrode was checked using four different electrodes for the analysis of 40.0 mM PMZ. The results showed a RSD% of 0.72% and 1.03% in  $I_p$  and  $E_p$  for oxidation of PMZ. Further, the stability of MWCNT-COOH@PGE was examined by storing of the electrode in the laboratory at room temperature and analysis of 25.0  $\mu\text{M}$  PMZ by DPV method daily. The results showed that the electrode signal retained upto 96.2% of its initial response after fifteen days. These results indicate good stability and reproducibility and repeatability of MWCNT-COOH@PGE for PMZ measurements.

#### Interference studies

The effect of some ions and molecules as potentially interfering compounds in the determination of PMZ was studied under the optimum conditions with 10.0  $\mu\text{M}$  PMZ at pH 4.0. To determine the interfering species, the concentration of the interfering ions or molecules was increased gradually until there was a  $\pm 5\%$  change in the oxidation current relative to the initial current. Results show that selectivity was not affected by 200-folds of tryptophan, tyrosine, glycine, alanine and phenyl alanine and 160-folds ascorbic acid (due to electrostatic repulsion with the surface). However, uric acid showed

interference at 12 fold concentration as compared to PMZ, which will allow simultaneous determination of PMZ and UA under optimum pH. Also, some ions such as  $\text{Zn}^{+2}$ ,  $\text{Mn}^{+2}$ ,  $\text{Al}^{+3}$ ,  $\text{Na}^+$ ,  $\text{Co}^{+2}$ ,  $\text{Cu}^{+2}$ ,  $\text{Li}^+$ ,  $\text{NO}_3^-$ ,  $\text{Cl}^-$  and  $\text{SO}_4^{-2}$  did not show any interference in the determination of PMZ.

#### Determination of PMZ in real samples

In order to demonstrate the application of the electrode for estimation of PMZ in real samples, the voltammetric determination of PMZ in anti-allergic cough syrup and human blood plasma samples was carried out. The anti-allergic cough syrup (1.0 mL) was added to 5.0 mL PBS (0.1 M, pH 4.0). Then 0.4 mL of this sample was added to a 25 mL buffer cell and standard addition method was applied. The values of experimentally determined PMZ were compared with the certified amount of PMZ in the syrup. Furthermore, the diluted human blood plasma sample was spiked with varying concentrations of PMZ and its DPV was plotted using the modified electrode. Recoveries were found to be in the range of 95.0–101.0% in the determination of PMZ in both the samples. The results are given in Tables S4 and S5 (Supplementary Data). These results demonstrated the ability of MWCNT-COOH@PGE for voltammetric determination of PMZ with high sensitivity in real samples.

#### Conclusions

A multiwalled carbon nanotube modified pencil graphite electrode (MWCNT-COOH@PGE) was electrochemically oxidized and used for the sensitive detection of trace amounts of PMZ. The modified electrode was investigated with the help of SEM and TEM, cyclic voltammetry and electrochemical impedance spectroscopy. The MWCNT-COOH@PGE showed good electrocatalytic activity for the oxidation of PMZ in two wide linear ranges (0.05–62.5  $\mu\text{M}$  and 62.5–275.0  $\mu\text{M}$ ) and a good detection limit (5.61 nM) for PMZ. This sensor was successfully applied to determine PMZ concentrations in pharmaceutical syrup and human blood serum samples.

#### Supplementary Data

Supplementary data associated with this article are available in the electronic form at [http://www.niscair.res.in/jinfo/ijca/IJCA\\_57A\(06\)770-777\\_SupplData.pdf](http://www.niscair.res.in/jinfo/ijca/IJCA_57A(06)770-777_SupplData.pdf).

#### References

- 1 Iijima S, *Nature*, 354 (1991) 56.
- 2 Baughman R H, Zakhidov A A & Heer W A, *Science*, 297 (2002) 787.

- 3 Musamech M, Wang J, Merkoci A & Lin Y H, *Electrochem Comm*, 4 (2002) 743.
- 4 Britto P J, Santhanam K S V, Rubio A, Alonso J A & Ajayan P M, *Adv Mater*, 11 (1999) 107.
- 5 Ye J S, Liu X, Cui H F, Zhang W D, Sheu F S & Lim T M, *Electrochem Commun*, 7 (2005) 249.
- 6 Saito T, Matsushige K & Tanaka K, *Physica B*, 323 (2002) 280.
- 7 Esumib K, Ishigamib M, Nakajimab A, Sawadab K & Hondab H, *Carbon*, 34 (1996) 279.
- 8 Li C, Wang D, Liang T, Wang X, Wu J & Hu X, *Powder Technol*, 142 (2004) 175.
- 9 Zhang Y f & Liu Z f, *J Phys Chem B*, 108 (2004) 11435.
- 10 Ebbesen T W, Ajayan P M, Hiura H & Tanigaki K, *Nature*, 367 (1994) 519.
- 11 Wang Y, Wu J & Wei F, *Carbon*, 41 (2003) 2939.
- 12 Tsang S C, Chen Y K, Harris P J F & Green M L H, *Nature*, 372 (1994) 159.
- 13 Tohji K, Goto T, Takahashi H, Shinoda Y, Shimizu N & Jeyadevan B, *Nature*, 383 (1996) 679.
- 14 Fang H T, Liu C G, Liu C, Li F, Liu M & Cheng H M, *Chem Mater*, 16 (2004) 5744.
- 15 Unger E, Graham A, Kreupl F, Liebau M & Hoenlein W, *Curr Appl Phys*, 2 (2002) 107.
- 16 Ito T, Sun L & Crooks R M, *Electrochem Solid State Lett*, 6 (2003) C4.
- 17 Honarmand E, Motaghedifard M H & Amani A M, *J Adv Med Sci Appl Tech*, 1 (2015) 61.
- 18 Wang J, Kawde A N & Sahlin E, *Analyst*, 125 (2000) 5.
- 19 Ozcan A, Sahin Y, *Biosens Bioelectron*, 25 (2010) 2497.
- 20 Keskin E, Yardım Y & Senturk Z, *Electroanalysis*, 22 (2010) 1191.
- 21 Sudeshna G & Parimal K, *Eur J Pharmacol*, 648 (2010) 6.
- 22 T Alizadeh & M Akhondian, *Electrochim Acta*, 55 (2010) 5867.
- 23 Marcoa J P, Borgesa K B, Tarley C R T, Ribeiro E S & Pereira A C, *Sensors Actuators B*, 177 (2013) 251.
- 24 Sultan S M, Hassan Y A M & Abulkibash A M, *Talanta*, 59 (2003) 1073.
- 25 Kosior M W, Skalska A & Matysik A, *J Pharm Biomed Anal*, 41 (2006) 286.
- 26 Quintana M C, Blanco M H, Lacal J & Hermández L, *Talanta*, 59 (2003) 417.
- 27 Le D C, Morin C J, Beljean M, Siouffi A M & Desbène P L, *J Chromatogr A*, 1063 (2005) 235.
- 28 Hassan A K, Saad B, Ghani S A, Adnan R, Rahim A A, Ahmad N, Mokhtar M, Ameen S T & Araj S M A, *Sensors*, 11 (2011) 1028.
- 29 Tang H, Chen J H, Cui K Z, Nie L H, Kuang Y F & Yao S Z, *J Electroanal Chem*, 587 (2006) 269.
- 30 Hinds B J, Chopra N, Rantell T, Andrews R, Gavalas V & Bachas L G, *Science*, 303 (2004) 62.
- 31 Curran S, Ellis A V, Vijayaraghavan A & Ajayan P M, *J Chem Physics*, 120 (2004) 4886.
- 32 Bard A J & Faulkner L R, *Electrochemical Methods. Fundamentals and Applications*, (Wiley, New York), 2001.
- 33 Felix F S, Ferreira L M C, Vieira F, Trindade G M, Ferreira V S S A & Angnes L, *New J Chem*, 39 (2015) 696.
- 34 Xiao P, Wu W, Yu J & Zhao F, *Int J Electrochem Sci*, 2 (2007) 149.
- 35 Pereira P F, Marra M C, Cunha R R, da Silva W P, Munoz R A A & Richter E M, *J Electroanal Chem*, 713 (2014) 32.
- 36 Ribeiro F W P, Cardoso A S, Portela R R, Lima J E S, Machado S A S, de Lima P, Souza D & Correia A N, *Electroanalysis*, 20 (2008) 2031.